Analysis of Weakly Coupled Neuronal Oscillators and Its Applications to Leech Swimming *

Zhiyong Chen
School of Electrical Engineering and Computer Science
The University of Newcastle
Callaghan, NSW 2308, Australia
zhiyong.chen@newcastle.edu.au

Tetsuya Iwasaki
Department of Mechanical and Aerospace Engineering
University of California
Los Angeles, CA 90095, USA
tiwasaki@ucla.edu

***Abstract*— This paper introduces a mathematical tool for analyzing neuronal oscillator circuits based on multivariable harmonic balance (MHB). The tool is applied to a model of the central pattern generator (CPG) for leech swimming, which comprises a chain of weakly coupled segmental oscillators. The results demonstrate the effectiveness of the MHB method and provide analytical explanations for some CPG properties.**

***Index Terms*— Neuronal networks, Central pattern generator, Harmonic balance, Coupled oscillators**

I. Introduction

The central pattern generators (CPGs) for rhythmic movements of animals during locomotion have been studied for decades. Physiological experiments [1] and mathematical modeling [2] have revealed how neuronal interconnections are made for CPGs of a variety of animals. In particular, mathematical modeling enables us to examine which system parameters determine dynamical properties of locomotion. One way to exploit a CPG model (differential equations) is to simulate the oscillatory behavior for various scenarios via numerical integration. However, simulations can be time consuming for a large network of neurons, and the underlying mechanisms for pattern generation are likely to remain hidden within the computer code. An alternative, complementary approach is mathematical analyses of the model. Such analyses could uncover direct and explicit relationships between a property of interest (e.g. phase) and system parameters, providing more insights into the oscillation mechanisms. Various theoretical analysis methods for understanding CPGs have been described in the literature including perturbation theory and averaging [3], Malkin theorem and phase coupled oscillator (PCO) model [4], and so on.

Another well-known method for the analysis of oscillators is the harmonic balance approach (see e.g. [5]) that approximates the oscillatory signals by sinusoids. Recently, the authors have developed a new framework called multivariable harmonic balance (MHB) to analyze CPGs consisting of multiple identical neuronal modules [6], [7]. The MHB method allows for a simple characterization of the oscillation profile — frequency, amplitude, bias, and phase, and it provides insights into pattern generation mechanisms. The main objectives of this paper are to (i) illustrate how the MHB method can be applied to the analysis of weakly coupled oscillators and demonstrate its effectiveness, and (ii) provide analytical explanations for some of the properties of the leech swimming CPG that were revealed earlier through physiological experiments [1] and model simulations [8].

*This work is partially supported by Australian Research Council Grant DP0878724 to Z. Chen and by NSF No.0654070 and ONR MURI Grant N00014-08-1-0642 to T. Iwasaki.

II. Problem Formulation

Many neuronal circuits that underlie animal locomotion comprise a combination series of local oscillators: [1]

$$v_k = \beta e + \mu M_k(s)\phi(v_k),\ k = 1, \cdots, m \tag{1}$$

where $v_k \in \mathbb{R}^n$ is the membrane potentials of n neurons within the segment, $\beta \in \mathbb{R}$ is a tonic stimulus from excitatory neurons (e.g., cell 204 for the leech swimming CPG [9]), and μ is the coupling strength of the intrasegmental connection. The function

$$\phi(x) := \max(x, 0). \tag{2}$$

represents the steady-state relationship between the presynaptic and postsynaptic potentials. The matrix $M_k(s) := f(\tau_k s)M$ is a transfer matrix capturing the dynamics of the neuronal couplings, where τ_k is the time constant of the synaptic connections within the k^{th} segment and it varies slightly from one segment to another. The nominal value τ_o can be chosen equal to either one of the τ_ks or their average value. Let $\Delta\tau_o := [\max_k(\tau_k) - \min_k(\tau_k)]/(m-1)$ be a nominal size of the variations in time constants. We assume that the variation is small, i.e., $\varepsilon := \Delta\tau_o/\tau_o \ll 1$. To the first order approximation in ε, we have

$$f(\tau_k s) = f(\tau_o s) + \varepsilon g_k(s),\ g_k(s) := \frac{\tau_k - \tau_o}{\Delta\tau_o}\tau_o s f'(\tau_o s),$$

which implies $M_k(s) = M_o(s) + \varepsilon\Delta_k(s)$ with $M_o(s) = f(\tau_o s)M$ and $\Delta_k(s) = g_k(s)M$.

[1] Throughout this paper, e is a column vector with all entries being 1, and a scalar function, e.g., ϕ, acts elementwise when its argument is a matrix or vector.

When the oscillators are coupled, the CPG model becomes

$$v_k = \beta e + \mu M_o(s)\phi(v_k) + \epsilon \sum_{l=1}^{m} \Delta_{kl}(s)\phi(v_l),\ k = 1, \ldots, m, \tag{3}$$

where $\Delta_{kk}(s) = (\varepsilon/\sigma)\Delta_k(s)$ is equal to the perturbation term within the segmental oscillator with $\sigma := \epsilon/\mu$, and where $\Delta_{kl}(s)$ with $l \neq k$ is the transfer matrix describing the dynamics and structure of the coupling from the l^{th} segmental oscillator to the k^{th} with

$$\Delta_{kl}(s) = e^{-|k-l|\tau_d s} M_{kl},\ M_{kl} = \begin{cases} M_A & (k < l \leq k + q_A) \\ M_D & (k - q_D \leq l < k). \end{cases}$$

The time constant τ_{d} is the time it takes for an action potential to travel from one segment to an adjacent segment. The small parameter ϵ represents the strength of the intersegmental coupling which is assumed much weaker than the intrasegmental coupling μ ($\epsilon \ll \mu$), that is, $\sigma \ll 1$. The parameters q_A (q_D) and M_A (M_D) are the ascending (descending) projection spans and coupling structures, respectively. With $v := \text{col}(v_1, \cdots, v_m)$, the m equations in (3) can be expressed compactly as follows:

$$v = \beta e + \mathcal{M}(s)\phi(v), \quad \mathcal{M}(s) = \mu \mathcal{M}_o(s) + \epsilon \Delta(s). \tag{4}$$

An essential assumption of the MHB approach is that the induced oscillations in (4) are close to sinusoids with the high frequency harmonic terms sufficiently suppressed through the low-pass property of the synaptic dynamics, that is,

$$v_p(t) \cong \mathfrak{a}_p[\sin(\varpi t + \mathfrak{c}_p) + \mathfrak{b}_p], \quad p = 1, \cdots, nm \tag{5}$$

where ϖ, $\mathfrak{a} = \text{col}(\mathfrak{a}_1, \cdots, \mathfrak{a}_{nm})$, $\mathfrak{b} = \text{col}(\mathfrak{b}_1, \cdots, \mathfrak{b}_{nm})$, and $\mathfrak{c} = \text{col}(\mathfrak{c}_1, \cdots, \mathfrak{c}_{nm})$ are the frequency, amplitude, bias, and phase vectors, respectively. Substituting (5) into (4) and solving for the parameters ϖ, $\mathfrak{a}$, $\mathfrak{b}$, and $\mathfrak{c}$, one can obtain an estimate for the oscillation profile of the CPG. This is the main idea of harmonic balancing. A standard method to avoid the difficulty caused by the nonlinear function (2) is to use the approximation:

$$\phi(\mathfrak{a}[\sin x + \mathfrak{b}]) \cong \mathfrak{a}[\kappa_1(\mathfrak{b}) \sin x + \kappa_2(\mathfrak{b})], \tag{6}$$

where the second and higher order harmonics on the right hand side are assumed small and neglected and the gain functions $\kappa_1(\mathfrak{b})$ and $\kappa_2(\mathfrak{b})$ are called the describing functions. With the approximations in (5) and (6), we obtain two algebraic equations called MHB equations as follows: [2]

$$\begin{aligned} &\mathcal{H}_1(\varpi, \mathfrak{h}, \mathfrak{b}) := [I - \mathcal{M}(j\varpi)\kappa_1(\mathcal{B})]\mathfrak{h} = 0, \\ &\mathcal{H}_2(\mathfrak{a}, \mathfrak{b}) := [\mathcal{B} - \mathcal{M}(0)\kappa_2(\mathcal{B})]\mathfrak{a} - \beta = 0, \\ &|\mathfrak{h}| = \mathfrak{a}, \quad \angle \mathfrak{h} = \mathfrak{c}, \quad \mathcal{B} = \text{diag}(\mathfrak{b}). \end{aligned} \tag{7}$$

[2]Throughout the paper, for a vector $x \in \mathbb{C}^n$, we define $y = |x|$ by $y_k = |x_k|$, and $\theta = \angle x$ by $\theta_k = \angle x_k$ for $k = 1, \ldots, n$.

The neuronal network (4) is expected to have an oscillation profile $(\varpi, \mathfrak{a}, \mathfrak{b}, \mathfrak{c})$ in the sense of (5), if $(\varpi, \mathfrak{h}, \mathfrak{b})$ is the solution to

$$\mathcal{H}(\varpi, \mathfrak{h}, \mathfrak{b}) := \begin{bmatrix} \mathcal{H}_1(\varpi, \mathfrak{h}, \mathfrak{b}) \\ \mathcal{H}_2(\mathfrak{a}, \mathfrak{b}) \end{bmatrix} = 0.$$

So, what follows is to investigate the solution to $\mathcal{H}(\varpi, \mathfrak{h}, \mathfrak{b}) = 0$ and hence to reveal the effects of the CPG parameters on the oscillation profile.

III. Main Results

Since each segmental oscillator in (1) is a slight perturbation of the nominal segmental oscillator defined by (3) with $\epsilon = 0$, the oscillation profile of the former would be close to that of the nominal oscillator. Moreover, since each oscillator in (3) receives small inputs from other oscillators due to the weak intersegmental coupling, it is reasonable to assume that the oscillation profile within each oscillator does not deviate significantly from that for the uncoupled case. Therefore, the intrasegmental oscillation profile of each segmental oscillator under intersegmental coupling is well approximated by that of the nominal oscillator. On the other hand, the weak coupling can coordinate the timing (or phase) of the segmental oscillators. This paper aims to find how this coordination happens.

Let (ω, a, b, ψ) be the oscillation profile of the nominal segmental oscillator (3) with $\epsilon = 0$. Then, its MHB equations become

$$0 = [I - \mu M_o(j\omega)\kappa_1(B)]\,\hbar, \quad \hbar = Ae^{j\psi}, \tag{8}$$

$$\beta e = [B - \mu M_o(0)\kappa_2(B)]\,a. \tag{9}$$

with $\hbar := Ae^{j\psi}$, $A := \text{diag}(a)$, and $B := \text{diag}(b)$. We see that the matrix $\mu M_o(j\omega)\kappa_1(B)$ has an eigenvalue 1 and an associated eigenvector $\hbar$. For further analysis later, we denote the normalized left eigenvector by $\ell \in \mathbb{C}^n$:

$$0 = \ell^* \left[I - \mu M_o(j\omega)\kappa_1(B)\right], \quad \ell^* \hbar = 1.$$

Remark 3.1: Under the uniformity assumptions $a = \mathfrak{a}e$ and $b = \mathfrak{b}e$ with $\mathfrak{a}, \mathfrak{b} \in \mathbb{R}$, equations (8) and (9) reduce to

$$0 = (\lambda I - \mu M)\hbar,\ \lambda := 1/(f(j\tau_o\omega)\kappa_1(\mathfrak{b})),\ \hbar := e^{j\psi},$$
$$0 = (\mathfrak{c}I - \mu M)e,\ \mathfrak{c} := (\mathfrak{b} - \beta/\mathfrak{a})/(f(0)\kappa_2(\mathfrak{b})),$$

respectively. Clearly, λ is an eigenvalue of μM and $\hbar$ (ℓ) is the associated (left) eigenvector. While such pairs are not unique, the result in [6] suggests that the maximal eigenvalue[3] contains the information of a *stable* oscillation.

In terms of the oscillation profile for the nominal segmental oscillator, the solution to the MHB equation $\mathcal{H}|_{\epsilon=0}(\varpi_o, \mathfrak{h}_o, \mathfrak{b}_o) = 0$ of the uncoupled CPG can be expressed as follows :

$$\varpi_o = \omega, \quad \mathfrak{h}_o = \alpha \otimes \hbar, \quad \mathfrak{b}_o = e \otimes b \tag{10}$$

[3]The maximal eigenvalue is defined to be the one with the largest imaginary part among those with the largest real part.

for an arbitrary vector α satisfying

$$\alpha \in \mathbb{C}^m,\ |\alpha| = e,\ \theta := \angle\alpha.$$

In other words, the uncoupled CPG is expected to have the following oscillation profile:

$$v_p(t) \cong a_i[\sin(\omega t + \theta_k + \psi_i) + b_i],\ p := (k-1)n + i,\quad k = 1, \cdots, m,\ i = 1, \cdots, n$$

where θ represents the intersegmental phases depending on the initial states of the segments.

As explained at the beginning of this section, the intrasegmental oscillation profile of the weakly coupled CPG (4) can be approximated as $\varpi \approx \varpi_o,\ \mathtt{h} \approx \mathtt{h}_o,\ \mathtt{b} \approx \mathtt{b}_o$. However, the weak coupling can coordinate the intersegmental phase θ. Next, we will propose an approach for estimating θ followed by two effective predictive formulae.

Assumption 1: The solution to the MHB equation $\mathcal{H}(\varpi, \mathtt{h}, \mathtt{b}) = 0$ of the coupled CPG satisfies

$$\varpi = \varpi_o + o(\epsilon),\ \mathtt{h} = \mathtt{h}_o + \epsilon\tilde{\mathtt{h}} + o(\epsilon),\ \mathtt{b} = \mathtt{b}_o + \epsilon\tilde{\mathtt{b}} + o(\epsilon)$$

for some $\tilde{\mathtt{h}}, \tilde{\mathtt{b}} \in \mathbb{R}^{nm}$. Moreover, the perturbation $\tilde{\mathtt{b}}$ is uniform over the chain, i.e.,

$$\tilde{\mathtt{b}} = \gamma \otimes \tilde{b} \tag{11}$$

for some $\gamma \in \mathbb{R}^m$ and $\tilde{b} \in \mathbb{R}^n$.

Theorem 3.1: *Under Assumption 1, the intersegmental vector α satisfies*

$$(\rho\Gamma - \nabla)\alpha = o(1),\ \nabla := L^*\Delta(j\omega)\kappa_1(\mathcal{B}_o)H \tag{12}$$

with

$$L := diag(\ell, \ldots, \ell),\ H := diag(\hbar, \ldots, \hbar)$$

for some $\rho \in \mathbb{C}$.

Proof: For the convenience, we define

$$\mathcal{B}_o := \mathrm{diag}(\mathtt{b}_o),\ \tilde{\mathcal{B}} = \mathrm{diag}(\tilde{\mathtt{b}}),\ \tilde{B} = \mathrm{diag}(\tilde{b}),\ \Gamma := \mathrm{diag}(\gamma),$$

and note $\kappa_i(\mathcal{B}) = \kappa_i(\mathcal{B}_o) + \epsilon\kappa_i'(\mathcal{B}_o)\tilde{\mathcal{B}} + o(\epsilon)$. Using the fact that $\mathcal{H}|_{\epsilon=0}(\varpi_o, \mathtt{h}_o, \mathtt{b}_o) = 0$, the coupled MHB equation $\mathcal{H}_1(\varpi, \mathtt{h}, \mathtt{b}) = 0$ becomes

$$\begin{aligned}&[\mu\mathcal{M}_o(j\omega)\kappa_1'(\mathcal{B}_o)\tilde{\mathcal{B}} + \Delta(j\omega)\kappa_1(\mathcal{B}_o)](\alpha \otimes \hbar)\\ &\quad = [I - \mu\mathcal{M}_o(j\omega)\kappa_1(\mathcal{B}_o)]\tilde{\mathtt{h}} + o(1).\end{aligned} \tag{13}$$

By the definitions of L and H, we have

$$L^*(I - \mu\mathcal{M}_o(j\omega)\kappa_1(\mathcal{B}_o)) = 0, \quad L^*H = I.$$

Multiplying (13) by L^* from the left,

$$(L^*\Upsilon H - \nabla)\alpha = o(1),$$

with $\Upsilon := -\kappa_1(\mathcal{B}_o)^{-1}\kappa_1'(\mathcal{B}_o)\tilde{\mathcal{B}}$. Using (11), we have

$$L^*\Upsilon H = \rho\Gamma, \quad \rho := -\ell^*\kappa_1(B)^{-1}\kappa_1'(B)\tilde{B}\hbar,$$

and hence (12). ∎

Remark 3.2: In (12), $o(1)$ is a small term as $\epsilon \to \infty$, ρ is the maximal eigenvalue of $\Gamma^{-1}\nabla$, and α is the corresponding eigenvector. An algorithm could be proposed for solving (12) for α, ρ, and Γ. In practice, however, a simpler but effective solution to (12) is obtained by approximately letting $\Gamma = I$, i.e.,

$$(\rho - \nabla)\alpha = 0, \tag{14}$$

so that ρ is the maximal eigenvalue of ∇ and α is the associated eigenvector. In this case, $|\alpha| = e$ may not always hold. Nevertheless, this approximate solution may be sufficient to give a reasonable estimate of the intersegmental phases as we will discuss for the leech CPG model.

Theorem 3.1 proposes an approximate method to analyze the intersegmental phase coordination for weakly coupled CPGs, which is the most important characteristic of pattern generation. Two effective formulae for estimating the intersegmental phase lag $\eta \in \mathbb{R}^{m-1}$,

$$\eta_k := \theta_k - \theta_{k+1},\ k = 1, \cdots, m-1,$$

are given below. We first consider the case where the segmental oscillators are identical (no period gradient) and then take the period gradient into account later.

Predictive Formula 1: *Consider a chain of many ($m \gg 1$) identical segmental oscillators, i.e., $\tau_k = \tau_o,\ k = 1, \cdots, m$, if the biases within the nominal oscillator are uniform ($b = \mathtt{b}e$), then the average phase lag can be predicted as follows:*

$$\begin{aligned}\eta_o \quad = \quad &\left[r_A \sum_{k=1}^{q_A}(k\eta_A - k^2\omega\tau_d) + r_D \sum_{k=1}^{q_D}(k\eta_D + k^2\omega\tau_d)\right]\\ &/\left[r_A \sum_{k=1}^{q_A} k^2 + r_D \sum_{k=1}^{q_D} k^2\right],\end{aligned} \tag{15}$$

where $r_A e^{j\eta_A} = \ell^* M_A \hbar$ and $r_D e^{j\eta_D} = \ell^* M_D \hbar$. If $q_A = q_D = q$ and $r_A = r_D$, this formula reduces to

$$\eta_o = \left(\frac{\eta_A + \eta_D}{2}\right)\left(\sum_{k=1}^{q} k\right)/\left(\sum_{k=1}^{q} k^2\right). \tag{16}$$

Derivation: In Theorem 3.1, the basic coupling matrix ∇ is given by

$$\nabla = \mathtt{k}\begin{bmatrix} 0 & \nabla_1 & \cdots & \nabla_{q_A} & & 0 \\ \nabla_{-1} & 0 & \nabla_1 & \ddots & \ddots & \\ \vdots & \nabla_{-1} & 0 & \nabla_1 & \ddots & \nabla_{q_A} \\ \nabla_{-q_D} & \ddots & \nabla_{-1} & 0 & \ddots & \vdots \\ & \ddots & \ddots & \ddots & \ddots & \nabla_1 \\ 0 & & \nabla_{-q_D} & \cdots & \nabla_{-1} & 0 \end{bmatrix}$$

where q_A and q_D are the intersegmental projection spans in the ascending and descending directions, respectively, $\mathtt{k}$ is defined by $\mathtt{k} := \kappa_1(\mathtt{b})$, and

$$\nabla_k := r_A e^{j(\eta_A - k\omega\tau_d)},\ \nabla_{-k} := r_D e^{j(\eta_D - k\omega\tau_d)}$$

for integers $k \geq 1$. To estimate the average phase lag, let us consider the limiting case where the oscillator chain is infinitely long ($m = \infty$). In this case, a generic row of the MHB equation $(\rho I - \nabla)\alpha = 0$ takes the following form:

$$\sum_{k=-q_D}^{q_A} \nabla_k \alpha_k = 0, \quad \nabla_0 := -\rho/\mathsf{k}. \tag{17}$$

Due to the uniformity of the intersegmental connections over the chain (that makes ∇ a Toeplitz matrix), the eigenvector α has the structure such that α_{k+1}/α_k is constant over k. Consequently, the intersegmental phase lag is uniform over the chain, and we may let $\alpha_k = re^{-jk\eta_o}$ where η_o is the intersegmental phase lag per segment. Substituting this expression for α_k into (17) and solving for ρ, we have

$$\begin{aligned} \rho &= \mathsf{k} r_A \sum_{k=1}^{q_A} e^{j(\eta_A - k(\eta_o + \omega\tau_d))} \\ &+ \mathsf{k} r_D \sum_{k=1}^{q_D} e^{j(\eta_D + k(\eta_o - \omega\tau_d))}. \end{aligned} \tag{18}$$

This is a parametrization of the set of infinitely many eigenvalues of the infinite matrix ∇ in terms of $\eta_o \in \mathbb{R}$. The profile of a stable oscillation can be estimated from the maximal eigenvalue, and hence we are interested in finding η_o such that $f(\eta_o) := \Re[\rho]$ takes its maximum value. Taking the derivative and setting it to zero, we have

$$\begin{aligned} \frac{f'(\eta_o)}{\mathsf{k}} \cong &\left[r_A \sum_{k=1}^{q_A} (k\eta_A - k^2\omega\tau_d) + r_D \sum_{k=1}^{q_D} (k\eta_D + k^2\omega\tau_d) \right] \\ &- \left[r_A \sum_{k=1}^{q_A} k^2 + r_D \sum_{k=1}^{q_D} k^2 \right] \eta_o = 0 \end{aligned}$$

where we used the approximation $\sin(x) \cong x$ for small x. Solving this equation for η_o, we obtain the formula (15). ■

Predictive Formula 2: *Consider a chain of many ($m \gg 1$) non-identical segmental oscillators, if the biases within the nominal oscillator are uniform ($b = \mathfrak{b}e$), then the intersegmental phase lag can be predicted as follows:*

$$\begin{aligned} \eta_k &= \eta_o + (\varepsilon/\sigma)(\Delta\tau_k/\Delta\tau_o)\varphi, \ \Delta\tau_k := \tau_{k+1} - \tau_k \\ \varphi &:= -\Im[\mathsf{k}(\ell^* M\hbar) j\tau_o \omega f'(j\tau_o\omega)/\rho] \end{aligned} \tag{19}$$

where η_o and ρ are given by (16) and (18), respectively.

Derivation: First, we assume that each segmental oscillator has the nominal time constant τ_o except that the p^{th} segment has the time constant $\tau_p \neq \tau_o$. With this change, the basic coupling matrix, denoted by $\bar{\nabla}$, is slightly modified from ∇ by $\bar{\nabla} = \nabla + \xi_p e_p e_p^{\mathsf{T}}$ where e_p is the vector having zero entries except for the p^{th} entry which is one, and ξ_p is defined as $\xi_p := \mathsf{k}(\varepsilon/\sigma)(\ell^* M\hbar) g_p(j\omega)$. Now, the MHB equation becomes $(\bar{\rho} I - \bar{\nabla})\bar{\alpha} = 0$. We assume that the effect of the time constant perturbation is local in the sense that $\bar{\alpha} \cong \alpha + e_p\delta_p$ for some $\delta_p \in \mathbb{C}$, where α is the maximal eigenvector of ∇ satisfying $\nabla\alpha = \rho\alpha$ for the eigenvalue ρ defined in (18). We further assume that the perturbation in the eigenvalue is small; $\bar{\rho} \cong \rho$. With these approximations, we have

$$(\rho I - \nabla - \xi_p e_p e_p^{\mathsf{T}})(\alpha + e_p\delta_p) \cong 0. \tag{20}$$

Multiplying the equation by e_p^{T} from the left and using $\nabla\alpha = \rho\alpha$, we obtain $\delta_p \cong \varsigma_p \alpha_p$, $\varsigma_p := \xi_p/\rho$ where $|\varsigma_p|$ is assumed small. As a result, we have

$$\theta_p = -p\eta_o + \Im(\varsigma_p), \quad \theta_k = -k\eta_o \ \text{ for } k \neq p. \tag{21}$$

To derive a formula for the phase lags in the case of an arbitrary period gradient, we consider the time constant perturbation in a single oscillator as before and start with (20). Taking the summation of (20) over $p = 1, \ldots, \infty$, we have $(\rho I - \nabla - \Xi)\delta - \Xi\alpha \cong 0$ where Ξ is the (infinite) diagonal matrix having entries ξ_p with $p = 1, \ldots \infty$, and δ and α are (infinite) vectors with entries δ_p and α_p, respectively. This equation implies $(\rho I - \nabla - \Xi)(\alpha + \delta) \cong (\rho I - \nabla)\alpha = 0$. Hence, if the coupling matrix ∇ is perturbed to $\nabla + \Xi$ due to the period gradient, the resulting phases are perturbed from $\angle\alpha$ to $\angle(\alpha + \delta)$ or $\angle\alpha + \Im(\varsigma)$. In summary, the intersegmental phases for general period gradients, perturbed from a nominal τ_o, are estimated as $\theta_k = -k\eta_o + \Im(\varsigma_k)$, $\varsigma_k := \xi_k/\rho$, Using the definition of $g_k(s)$, we obtain (19). ■

IV. Application to Leech Swimming CPG

In this section, Theorem 3.1 and the two predictive formulae are applied to leech swimming CPGs that are described as a set of weakly coupled oscillators (4) with the following nominal parameters (perturbed cases are also considered):

$$f(\tau s) = \frac{1-r}{1+(1-r)\tau s}, \ M = \begin{bmatrix} 0 & -1 & 0 \\ 0 & 0 & -1 \\ -1 & 0 & 0 \end{bmatrix},$$

$$M_A = \begin{bmatrix} 0 & -1 & 0 \\ 0 & 0 & -1 \\ 0 & 0 & 0 \end{bmatrix}, \ M_D = \begin{bmatrix} 2 & 0 & 0 \\ 0 & 0 & 0 \\ 0 & 0 & 0 \end{bmatrix},$$

$$n = 3, \ m = 17, \ \tau_o = 200 \text{ ms}, \ r = 0.3, \ q = 5,$$

$$\tau_d = 15 \text{ ms}, \ \mu = 6, \ \beta = 30r \text{ mV}, \ \sigma := \epsilon/\mu = 0.015.$$

In what follows, we will make predictions on the intersegmental phase θ using (14), and compare the results with existing observations made from physiological experiments. The two predictive formulae developed in the previous section will explain the phase setting mechanisms underlying the experimental observations.

A. Effects of the projection span

First, we will examine how the intersegmental phase lags depend on the length of the oscillator chain, assuming that all the segmental oscillators are identical ($\tau_k = \tau_o$ for all k). Fig. 1 shows the relationship between the estimated phase lags and the number of ganglia in the chain, in comparison

with the experimental data from Fig. 3 of [10]. The average value of the intersegmental phase lags per segment is 30° for two segments, and reduces to about 8° as the number of segments increases. We note that the significant decrease occurs when the number of segments increases from two to six, and the average phase lag remains roughly constant beyond six. This tendency agrees with the data. Previous experimental observations [10] suggested that the intersegmental couplings spanned over about six segments (or the projection span was $q = 5$) but not more than seven segments. Given this fact, we hypothesize that the reduction in phase lag is related to the projection span, rather than the length of the oscillator chain. This hypothesis might be verified in the following table.

m	2	5	8	11	14	17
$q = 1$	30°	30°	30°	30°	30°	30°
$q = 3$	n.a.	14.9°	13.8°	13.4°	13.3°	13.2°
$q = 5$	n.a.	n.a.	9.6°	9.0°	8.7°	8.6°
$q = 7$	n.a.	n.a.	7.3°	7.0°	6.7°	6.5°

The predictive formula (16) for η_o clearly explains the dependence of the average phase lag on the projection span q. In particular, it shows that the average intersegmental phase lag η_o is a decreasing function of the connection span q since the denominator grows faster than the numerator as q gets larger. The following table, derived from (16), summarizes how η_o for the leech CPG changes with q:

q	1	2	3	4	5
η_o	30°	18°	13°	10°	8°

It confirms that the formula indeed captures the average phase lag.

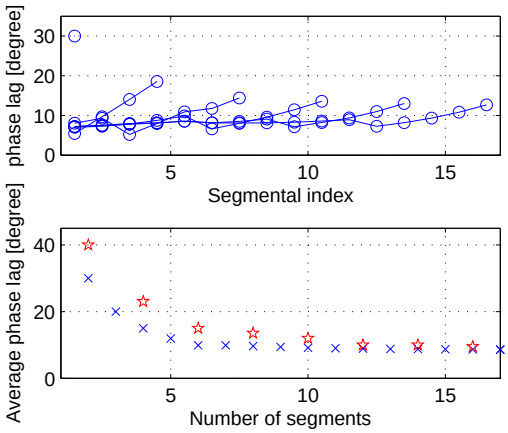

Fig. 1. Intersegmental phase lags of leech swimming CPGs composed of different numbers of segments ($m = 2, 5, 8, 11, 14, 17$) ($r = 0.3, \mu = 6, \sigma = 0.015, \tau_k = 200\text{ms}, \tau_d = 15\text{ms}$). Each line connecting $\circ$ (not a line but a single point for the case with $m = 2$) represents the phase lags of a segment with respect to its adjacent segment on the anterior side. The average phase lag is marked by $\times$ in the bottom graph for $m = 2, \cdots, 17$. The $\star$'s represent the physiological experiment results cited from [10].

The intersegmental phase lag can be further studied for the case where $q_A \neq q_D$ as in (15). Fig. 2 shows the phase lag curve for the nominal case ($q = 5$) as well as perturbed cases. The phase lags are found insensitive to q_D, but uniformly decrease when q_A is increased. This property is captured by the formula (15) that gives estimates as follows:

q_A	5	5	5	4	5	6
q_D	4	5	6	5	5	5
η_o	7.5°	8.2°	8.8°	10.2°	8.2°	6.0°

The estimates are quantitatively close to the average values of the phase lags in Fig. 2, indicating that the formula (15) obtained for an oscillator chain of infinite length approximates the average phase lag of a finite chain reasonably well.

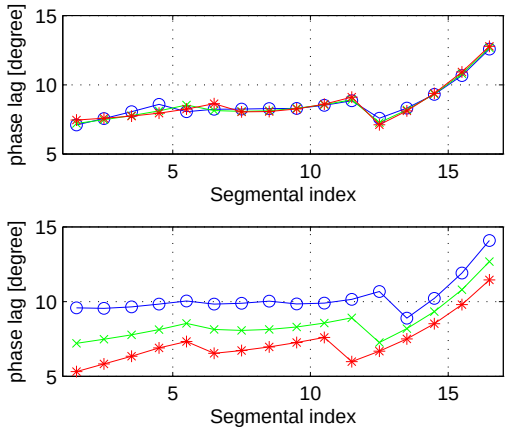

Fig. 2. The effects of the intersegmental projection span on the intersegmental phase lags ($r = 0.3, \mu = 6, \sigma = 0.015, \tau_k = 200\text{ms}, \tau_d = 15\text{ms}$). In the upper graph, the ascending projection span is fixed as $q_A = 5$ and the descending projection span q_D is varied from 4 to 6 ($\circ = 4$, $\times = 5$, and $* = 6$). In the lower graph, the descending projection span is fixed as $q_D = 5$ and the ascending projection span q_A is varied from 4 to 6. The locations of the two "edges" in each phase lag curve correlate exactly to the projection spans.

B. Effects of the period gradient, coupling strength, and communication delay

It has been found [11] that the segmental oscillators in the leech swimming CPG are not exactly identical to each other, but have differing intrinsic cycle periods. In this section, we will use the MHB approach to analyze how the period gradient and the coupling strength interplay to affect the intersegmental phase lag.

We consider the uniform period gradient case where the intrinsic periods of the segmental oscillators vary linearly along the body. In particular, we picked the time constant of the middle segment as the nominal value, i.e., $\tau_o = \tau_9 = 200$ ms, and set $\tau_k = (k - 9)\Delta\tau_o + \tau_o$ for a constant gradient $\Delta\tau_o$. From (19), the intersegmental phase lags would depend on $\varepsilon/\sigma := \Delta\tau_o/(\tau_o\sigma)$. Therefore, we examine the intersegmental phase lag curve for several cases where ε/σ

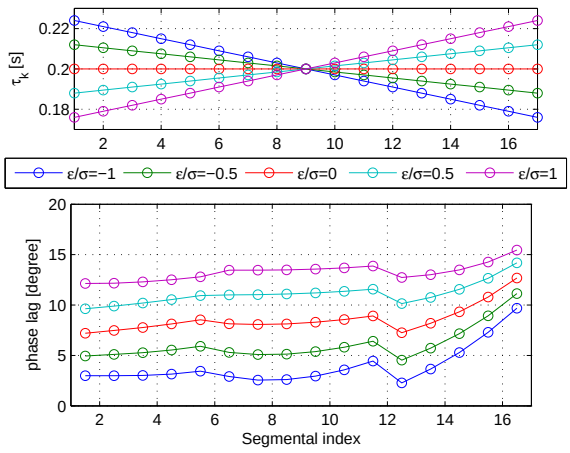

Fig. 3. Intersegmental phase lag curves with uniform period gradient ($r = 0.3, \mu = 6, \tau_d = 15\text{ms}$). The bottom graph depicts the phase lag curves for the cases $\varepsilon/\sigma = \pm 1, \pm 0.5$, and 0. The intersegmental phase lag η increases with ε/σ. For reference, the time constant τ_k of each segment is plotted in the upper graph for a particular choice $\sigma = 0.015$, where the slope $\Delta\tau_o$ varies between ± 3 ms so that ε/σ varies between ± 1.

takes a value between ± 1 in Fig. 3. It explains earlier observations from physiological experiments on leeches [12]: "For those ganglion chains in which the anterior ganglia had greater periods (i.e., $\varepsilon < 0$), the reduced coupling (σ) led to reduced or even reversed phase relationships (η) across the lesion. In contrast, reduced coupling (σ) between halves of a chain in which the posterior ganglia had greater cycle periods (i.e., $\varepsilon > 0$) led to increased phase lags (η) across the lesion." These observations correspond to the fact that, in (19), reduction in the coupling strength $\sigma > 0$ leads to a reduced/increased phase lag when the period gradient $\Delta\tau_k$ is negative/positive.

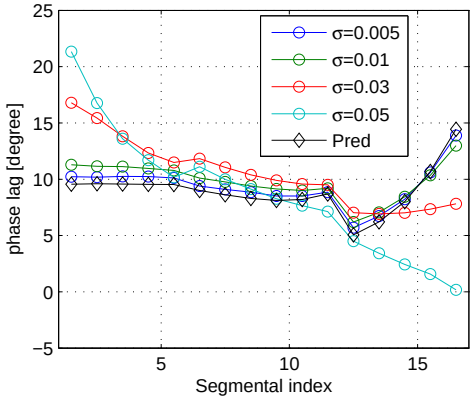

Fig. 4. Simulated and predicted intersegmental phase lags ($r = 0.3, \mu = 3, \tau_k = 200\text{ms}, \tau_d = 15\text{ms}$). The intersegmental coupling strength σ was varied from 0.005, 0.01, 0.03 to 0.05, and the model was simulated numerically, to obtain the phase lag curves marked by $\circ$. The phase lag curve predicted by the equations (12) is marked by $\diamond$. The predicted curve is independent of σ due to $\Delta\tau = 0$. The prediction error becomes more significant for a larger σ.

It is known [13] that it takes about $\tau_d = 15$ ms for an action potential to travel through the nerve cord from one segment to the next. This communication delay may have a significant impact on the intersegmental phase lags. In (19), when the communication delay τ_d is varied, the value of φ increases with τ_d almost linearly in the range $0 \le \tau_d \le 30$ ms, and can be approximated by $\varphi \cong \tau_d/10$ deg where the unit for τ_d is ms. Hence, from (19), we expect that the phase lags increase/decrease with τ_d in the presence of positive/negative time constant gradient $\Delta\tau_o$, but is insensitive to τ_d if the intrinsic periods are uniform over the oscillator chain. This property has been observed in simulation which is omitted due to space limitation.

Finally, the accuracy of MHB prediction is examined in Fig. 4 where the phase lag curves from numerical computer simulations for various values of σ are plotted in comparison with the phase lag curve predicted from analyses. The MHB analysis provides a very reliable prediction when the intersegmental coupling is weak as assumed in the analysis.

V. Conclusion

In this paper, an MHB method for oscillation analysis has been introduced and applied for a leech swimming CPG model. The leech CPG model was analyzed to estimate the intersegmental phase lags, exploiting the weakly coupled chain structure. Simple formulas are obtained for the average phase lag and for the phase lags with period gradient. These formulae and numerical analyses revealed how the intersegmental phase lags were determined by various parameters.

References

[1] W.B. Kristan Jr., R. Calabrese, and W.O. Friesen. Neuronal control of leech behavior. *Prog. in Neurobiol.*, 76:279–327, 2005.

[2] G.N. Orlovsky, T.G. Deliagina, and S. Grillner. *Neuronal Control of Locomotion: From Mollusc to Man*. Oxford University Press, 1999.

[3] M. Farkas. *Periodic Motions*. Springer-Verlag, 1994.

[4] E.M. Izhikevich. *Dynamical Systems in Neuroscience: The Geometry of Excitability and Bursting*. Cambridge, MA, The MIT Press, 2006.

[5] H.K. Khalil. *Nonlinear Systems*. Prentice Hall, 1996.

[6] T. Iwasaki. Multivariable harmonic balance for central pattern generators. *Automatica*, 44(12):4061–4069, 2008.

[7] Z. Chen and T. Iwasaki. Matrix perturbation analysis for weakly coupled oscillators. *Systems & Control Letters*, 58(2):148–154, 2009.

[8] M. Zheng, W.O. Friesen, and T. Iwasaki. Systems-level modeling of neuronal circuits for leech swimming. *J. Computational Neuroscience*, 22(1):21–38, 2007.

[9] E.A. Debski and W.O. Friesen. Role of central interneurons in habituation of swimming activity in the medicinal leech. *J. Neurophysiol.*, 55(5):977–994, 1986.

[10] R.A. Pearce and W.O. Friesen. Intersegmental coordination of the leech swimming rhythm. II. Comparison of long and short chains of ganglia. *J. Neurophysiol.*, 54:1460–1472, 1985.

[11] C.G. Hocker, X. Yu, and W.O. Friesen. Functionally heterogeneous segmental oscillators generate swimming in the medicinal leech. *J. Comp. Physiol.*, 186(9):871–883, 2000.

[12] R.A. Pearce and W.O. Friesen. Intersegmental coordination of the leech swimming rhythm. I. Roles of cycle period gradient and coupling strength. *J. Neurophysiol.*, 54:1444–1459, 1985.

[13] W.O. Friesen, M. Poon, and G.S. Stent. Neuronal control of swimming in the medicinal leech IV. Identification of a network of oscillatory interneurones. *J. Exp. Biol.*, 75:25–43, 1978.